A DYNAMIC REAL TIME MODEL FOR AIR-TO-AIR REFUELING

Per Weinerfelt and Andreas Nilsson
Saab Aerosystems, Flight Physics
SE-58188 Linköping
Keywords: *Aerial Refueling, Real time simulation models*

Abstract

The paper describes an Air-To-Air refueling simulation model which has been developed at Saab Aerosystems. The models have been developed from fundamental theory for structure mechanics, aerodynamics and flight mechanics. Verifications of the models have been done by comparison with data from video recording of air-to-air refueling.

1 Introduction

In recent years, Sweden's defense force has focused more on international participation. Besides taking part in the partnership for peace program, the Swedish air force has its SWAFRAP (Swedish Air Force Rapid Reaction Unit) JAS 39 team and it also participates regularly in international exercises. During international operations wide range flights and long sustainability are important. To meet these requirements the ability to perform Air-To-Air refueling has been introduced in the JAS 39 Gripen C/D.

For a few years a project has been ongoing at Saab Aerosystems aimed at developing AAR simulation capability. A largest part of the project has focused on modeling of the aerodynamics and flight mechanics part of the Air-To-Air refueling process with the JAS 39 Gripen C/D as the refueling aircraft and C130 Hercules as the tanker aircraft (see fig. 1 and 2). The main objective of the project is to provide simulation and visualization tools which can be used for studies and training of Air-To-Air refueling.

The impact from flow features behind the tanker aircraft, such as wing tip vortices and propeller slip stream, on the drogue, the hose and the refueling aircraft has been considered in the models. The fact that the flow field from the refueling aircraft is affecting the motion of the drogue and the hose has been taken into account. A sub model describing the docking mechanism is also included in the simulation system.

Fig. 1 Aerial refueling of a Gripen fighter behind a tanker.

Fig.2 Aerial refueling, two Gripen fighters behind an C130 Hercules

2 Mathematical and Physical models

The sections below describe the different sub models which are the basic part of the total simulation model.

2.1 Wing tip vortex model

A wing tip vortex model was developed earlier in an internal Saab project. This model has to a large extent been reused in the present work. The model has been used to generate wing tip vortex field behind the aircraft C130 Hercules. Aircraft-specific parameters in the model are the wing span, the wing chord, the lift coefficient and the speed of the aircraft.
A complete delta aero data base for the Gripen fighter has been calculated using a linear panel method. Figure 3 below shows a typical velocity field from two wake vortices. Aerodynamic loads and moments, from the wake vortices, on the hose and basket are calculated directly total velocity field i.e. the sum of the velocity contribution from the vortex model and the velocity of the tanker aircraft.

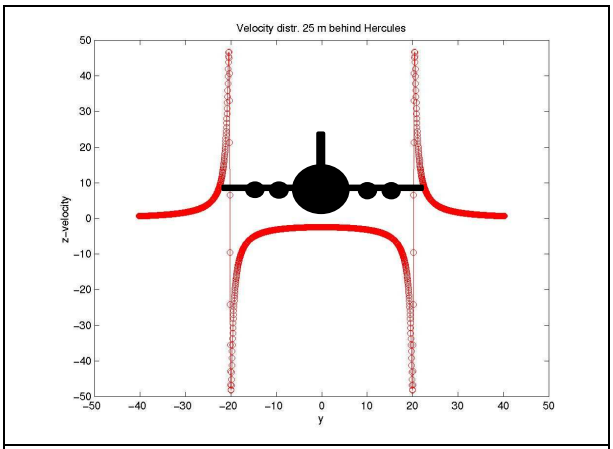

Fig. 3. Velocity field, from wing tip vortices, behind a tanker aircraft.

2.2 Wing tip vortex model

The refueling Gripen aircraft is affected by wing tip vortices as well as the propeller slip stream from the propellers of, in our study, a C130 Hercules. The slip stream model we have developed consists of follow essential parts:

1. Calculation of the mean value, over the rotor disk, of the axial velocity contribution V_x using momentum theory. (i.e. equations describing the conservation of mass and momentum across the rotor disk).

2. A continuous velocity distribution, over the rotor disk, is created by scaling a typical velocity distribution from wind tunnel test so that the average value is the same as in 1 above. (see Figure 4).

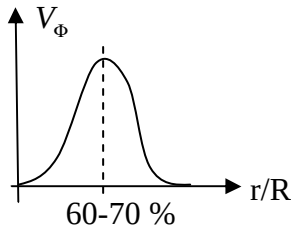

Fig. 4. Typical radial velocity distribution V_Φ, over the propeller disk.

3. Calculation of the tangential velocity V_Φ using V_x above and propeller theory (see Figure 5).

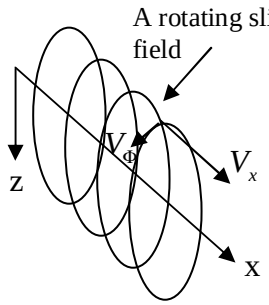

Fig.5. Slip stream field and velocity components V_x och V_Φ

4. Correction of the slip stream propagation direction by using rigid body mechanics applied to a rotating solid circular disk (see Figure 6).

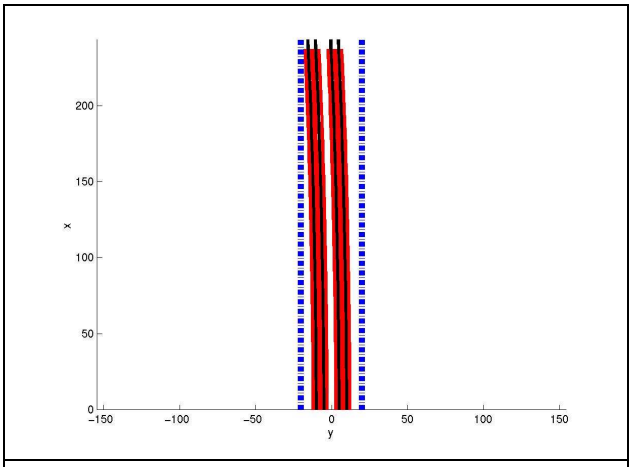

Fig. 6 Computed slip stream and wing tip vortex paths behind a propeller aircraft.

Figure 7 shows the total forces and moments generated on an aircraft traversing through a wing tip vortex and slip stream field. It should be pointed out that impact from this flow field can be neglected at the position where air refueling normally takes place i.e. at 5-10 m below the tanker aircraft (assuming a hose length of 30 m).

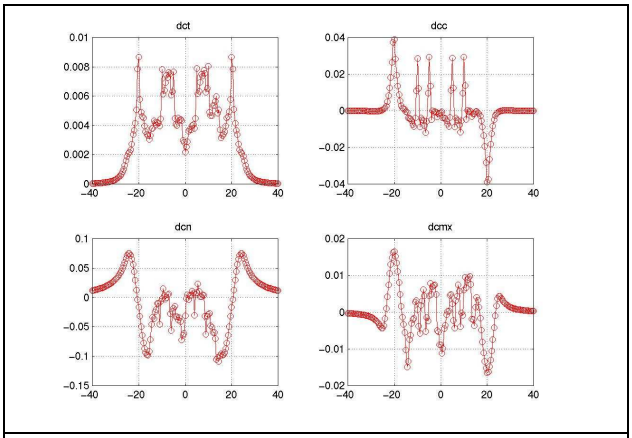

Fig. 7. Incremental forces and moments on an incoming aircraft traversing through the a wing tip vortex and slip stream field at z=1 m.

2.3 Velocity field around the incoming aircraft

The velocity field in a box with size 10x10x5 m around the incoming aircraft has been calculated by solving the Euler equations (inviscid flow). Computed velocity data for different speeds, angles of attack and side slip angles are stored in tables. The velocity increment on the tube and the basket is then determined by linear interpolation using these tables. Figure 8 shows the Gripen aircraft and the sample points at which the speed is calculated. The velocity outside the box is zero.

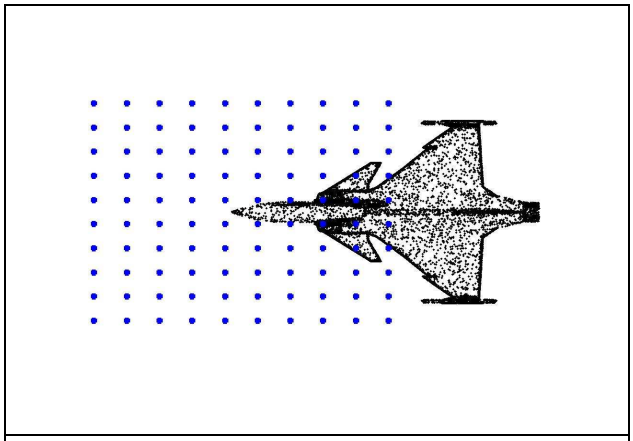

Fig. 8. Flow field box around the incoming aircraft.

2.3 Aerodynamic forces on the hose

We consider a tube in Figure 9 which is surrounded by a velocity field which is parallel to the x-axis and has magnitude V. The model we are using for calculating the aerodynamic forces on the hose is based on a decomposition of the velocity in a tangential and a normal part (relatively to the hose). We assume that the tangential and normal forces can be calculated independently by applying the formula

$F = \frac{\rho U^2}{2} S_{ref} c_F$ in the two directions. Here $\frac{\rho U^2}{2}$ is the dynamic pressure, S_{ref} the reference area and c_F the force coefficient.

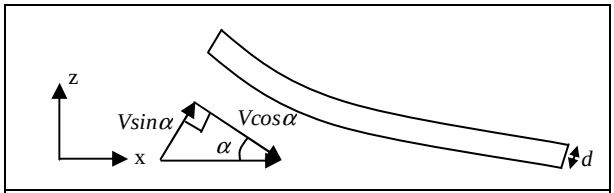

Fig 9. The hose and velocity components

For the tangential force per length unit holds

$$f_{ta} = \frac{\rho V^2 \cos^2 \alpha}{2} \pi d c_{ft} \qquad (1)$$

where

$$c_{ft} = c_{ft}(s, \mathrm{Re}_s),\ \mathrm{Re}_s = \frac{s\rho V\cos\alpha}{\mu}$$

and the normal force per length unit is determined by

$$f_{na} = \frac{\rho V^2 \sin^2\alpha}{2} dc_{fn} \qquad (2)$$

where

$$c_{fn} = c_{fn}(\mathrm{Re}_n),\ \mathrm{Re}_n = \frac{d\rho V\sin\alpha}{\mu}$$

The letter *s* denotes the arc length, ρ the air density and μ air viscosity. The force coefficients c_{ft} och c_{fn} can be estimated by corresponding ones for the flow over a flat plate and a circular cylinder respectively. Typical values c_{ft} and c_{fn} are c_{ft}=0.0045 and c_{fn}=1.0. We assume furthermore that the diameter *d* of the hose is much shorter that the length *L*.

2.3 Aerodynamic forces on the basket

We simplify the real basket by considering a conical rotational symmetric basket in a velocity field according to Fig. 10.

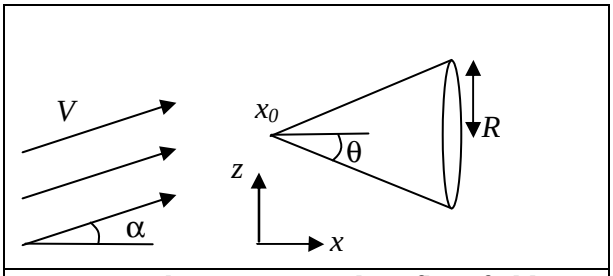

Fig. 10 Basket an surrounding flow field

Aerodynamic drag and lift can then be expressed according to

$$D = \frac{\rho V^2}{2} S_{ref} C_d \ \text{ and } \ L = \frac{\rho V^2}{2} S_{ref} C_{L,\alpha}\alpha,$$

where S_{ref} is a reference area which here will be the base area of the basket i.e. $S_{ref} = \pi R^2$.

The forces in the *x* and *r* direction are computed from the equations

$$\begin{cases} F_x = D\cos\alpha - L\sin\alpha \\ F_r = D\sin\alpha + L\cos\alpha \end{cases} \qquad (3)$$

Flight test data from aerial refueling with the F18 combined with experiments on badminton balls leads to following estimation of the drag and lift coefficients C_d and $C_{L,\alpha}$, $C_d \approx 0.556$ and $C_{L,\alpha} \approx 0.382$ (se ref. 3 and 5).

The torque M_0 around the point x_0 in figure 10 can be written,

$$M_{0,a} = \frac{\rho V^2}{2} S_{ref} R C_{M,\alpha}\alpha \ \text{ where } C_{M,\alpha} \approx -0.174.$$

2.4 The equations of motion of the hose

The dynamic equations of the hose are given by the Newton's law according to

$$\begin{cases} \rho AL\ddot{x} = F_x \\ \rho AL\ddot{y} = F_y \\ \rho AL\ddot{z} = F_z \end{cases} \qquad (3)$$

ρ is the density of the hose, *A* cross-sectional area, *L* the length of the hose, *x*, *y*, *z*, the displacement of the hose and F_x, F_y, F_z components of total force, acting on hose. The total force is split up in an aerodynamic force, elastic forces in the hose and a gravity force according to

$$\begin{cases} \Delta F_x = \Delta f_{elast,x} + \Delta f_{areo,x} + \Delta l f_{0,x} \\ \Delta F_y = \Delta f_{elast,y} + \Delta f_{areo,y} + \Delta l f_{0,y} \\ \Delta F_z = \Delta f_{elast,z} + \Delta f_{areo,z} + \Delta l f_{0,z} - \rho A\Delta l\, g \end{cases} \qquad (3)$$

The elastic force components can furthermore be expressed according to

$$\begin{aligned} \Delta f_{elast,x} &= \Delta l EA\frac{\partial\varepsilon}{\partial l} = E\pi\left(r_1^2 - r_0^2\right)\Delta l\frac{\partial\varepsilon}{\partial x}, \\ \Delta f_{elast,y} &= \Delta l EI_{yy}\left[-\frac{\partial^2\kappa_y}{\partial l^2}\right] = E\pi\frac{\left(r_1^4 - r_0^4\right)}{4}\Delta l\left[-\frac{\partial^2\kappa_y}{\partial l^2}\right] \\ \Delta f_{elast,z} &= \Delta l EI_{zz}\left[-\frac{\partial^2\kappa_z}{\partial l^2}\right] = E\pi\frac{\left(r_1^4 - r_0^4\right)}{4}\left[-\frac{\partial^2\kappa_z}{\partial l^2}\right] \end{aligned} \qquad (4)$$

where ρ is the density of the hose, *A* the cross sectional area of the hose, Δl a length increment along the hose, *x*,*y*,*z*, displacements, κ_y, κ_z the hose curvature in the *y*,*z* direction, ε the strain, E the elasticity module, r_1 and r_0 the inner and outer radius of the hose. Assuming relatively small deformation the curvature and strain can

be approximated by $\kappa_y = \frac{\partial^2 y}{\partial l^2}$, $\kappa_z = \frac{\partial^2 z}{\partial l^2}$, $\varepsilon = \frac{\partial x}{\partial l}$ which leads to final form of the dynamic hose equations

$$\begin{aligned}
\ddot{x} &= \frac{E}{\rho}\frac{\partial^2 x}{\partial l^2} + \frac{f_{a,x}}{\rho A} + \frac{f_{0,x}}{\rho A} \\
\ddot{y} &= \frac{E}{\rho}\frac{\left(r_1^2 + r_0^2\right)}{4}\left[-\frac{\partial^4 y}{\partial l^4}\right] + \frac{f_{a,y}}{\rho A} + \frac{f_{0,y}}{\rho A} \\
\ddot{z} &= \frac{E}{\rho}\frac{\left(r_1^2 + r_0^2\right)}{4}\left[-\frac{\partial^4 z}{\partial l^4}\right] + \frac{f_{a,z}}{\rho A} + \frac{f_{0,z}}{\rho A} - g
\end{aligned} \qquad (5)$$

The force f_0 is the contact force between the hose and basket. Equation (5) is discretized in space by FEM i.e. the displacements are approximated by

$$\begin{aligned}
x(l,t) &= \sum c_{k,x}(t) B_{k,x}(u) \\
y(l,t) &= \sum c_{k,y}(t) B_{k,y}(u) \\
z(l,t) &= \sum c_{k,z}(t) B_{k,z}(u)
\end{aligned} \qquad (6)$$

where $u=l/L$ is a length parameter $0 \le u \le 1$. The basis functions $B_{k,x}$, $B_{k,y}$, $B_{k,z}$ are eigen functions to following differential equations

$$\begin{aligned}
\frac{E}{\rho L^2}\frac{d^2 B_{k,x}}{du^2} &= \lambda_{k,x} B_{k,x}, \\
\frac{E}{\rho L^4}\frac{\left(r_1^2 + r_0^2\right)}{4}\frac{d^4 B_{k,y}}{du^4} &= -\lambda_{k,y} B_{k,y}, \\
\frac{E}{\rho L^4}\frac{\left(r_1^2 + r_0^2\right)}{4}\frac{d^4 B_{k,z}}{du^4} &= -\lambda_{k,z} B_{k,z}
\end{aligned} \qquad (7)$$

Equation (6) inserted into (5) yield a system of time dependent ordinary differential equation where the coefficients $c_{k,x}, c_{k,y}, c_{k,z}$ are the unknowns. These nonlinear equations are linearized around the steady state solution to the nonlinear problem. An implicit Runge-Kutta method, which is unconditional stable, is used to approximately solve the linear system.

2.4 The equations motion of the basket

We consider the basket as rigid body and hence apply rigid body mechanics to the basket. The forces and moment equations are expressed in a body fixed coordinate system.

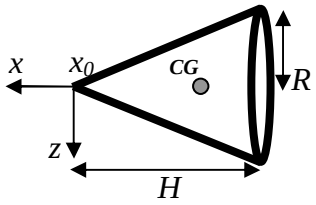

Fig 11. Basket fixed coordinate system

The moment or torque equation around the contact point x_0 reads

$$I_0 \dot{\omega}_B + \omega_B \times (I_0 \omega_B) = M_0 - m_k x_{0CG} \times (A_{E2B} \ddot{x}_0) \qquad (8)$$

where I_0 is moment of inertia, around x_0, for the basket, and m_k the basket mass. Equation (8) is the dynamic equation describing the motion of the basket. The moment M_0 includes all moments acting on the basket which can be written

$$M_0 = M_{0,a} + x_{0i} \times F_i + m_k (x_0 - x_{CG}) \times F_{gravity} \qquad (9)$$

where $M_{0,a}$ is the aerodynamic moment around x_0. The only missing equation, which connects the hose and tube, is the relation between the contact force F_0 and the acceleration of the end point of the hose $\ddot{x}_0$. This equation is obtained from the force equation of the basket

$$\begin{aligned}
&m_k \dot{\omega}_B \times (x_0 - x_{CG}) = F_a + F_0 + F_i + m_k A_{E2B} \bar{g} - \\
&m_k A_{E2B} \ddot{x}_0 - m_k (\omega_B \times (\omega_B \times (x_0 - x_{CG})))
\end{aligned} \qquad (10)$$

In each time step, in the numerical integration of equation of motion for the hose and basket, the data of F_0 and $\ddot{x}_0$ are exchanged between the hose and basket.

A sub model describing the docking mechanism is also included in the simulation system.

3 Code implementation and results

The different sub models, described above, has been encoded, first in MATLAB and later on in FORTRAN, and then validated and verified. For instance, the dynamics of the hose has been compared with the dynamics of a swaying slender beam having an elasticity module of the same order as the hose. Furthermore, the shape and bending of the hose has been compared with video-sequences taken during actual air-to-air refuelling missions. The conclusion is that the behaviour of the model is well in agreement with what can be observed in the videos. The dynamics of the basket has been validated by comparison with studies of the behaviour of shuttlecocks (see ref. [5]). After validating the separate models, they were put together in a coupled system, which in turn was verified to provide realistic output. The verification was done on a hose and basket exposed to disturbances of an incoming aircraft. Finally, all the sub models have been integrated into ARES, a 6 DOF flight simulation program developed and used by Saab. By extracting data from desktop tests with ARES we could verify that the integrated system behave as could be expected from our tests of the separate sub models. The next step will be to integrate the program in a true flight simulator. First various parameters will be tuned and then the system will be tried out by a pilot.

The difference between performing a desktop simulation with ARES and using a flight simulator is mainly that in the latter case the position and motion of the tanker aircraft is provided from outside as in-signals to the system. While in a desktop simulation they are implemented in the program. In practice this implies that the interaction will be less complex during a desktop simulation. You tend to fly in straight lines and so on.
To speed up the interface between the computer performing the simulation and the computers used to visualize in the flight simulator, the implementation is made so that only the coefficients in the system (6) need to be sent. An example of results obtained from the simulation model is shown in figure 12. The figure (top) shows a realistic motion, in the y-direction, of the basket due to an incoming aircraft approaching the basket. The position of the incoming aircraft relatively to the basket is plotted in the bottom of figure 12.

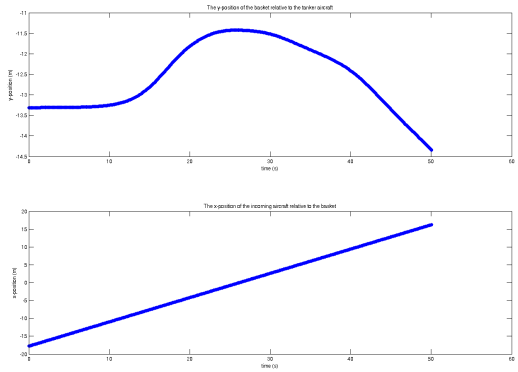

Fig 12. Motion of the basket due to an incoming aircraft.

4 References

[1] Y. Sedin et.al. ”A model for simulation of flight passages through trailing edge tip vortices”, *paper ICAS 3003-7.9.3, in the proceedings to the ICAS 2002 conference.*

[2] Y. Sedin. ”Preliminary studies of simulation models for aerial refueling”. *Saab report, TDA-2004-0179.*

[3] Y. Sedin. “Preliminary studies and private communications”

[4] P. Weinerfelt, “Mathematical and Physical models for simulation of aerial refueling”. *Saab report, TDA-2008-0030.*

[5] A. J. Cooke, “Aerodynamics and Mechanics of Shuttlecocks”, Ph. D. thesis, Department of Engineering, University of Cambridge, 1992.

Copyright Statement